Momentum spectra of electrons rescattered from rare-gas targets following their extraction by one- and two-color femtosecond laser pulses

D. Ray,[1] Zhangjin Chen,[1] S. De,[1] W. Cao,[1] I. V. Litvinyuk,[1,2] A. T. Le,[1] C. D. Lin,[1] M. F. Kling,[1,3] and C. L. Cocke[1]

[1]*J. R. Macdonald Laboratory, Physics Department, Kansas State University, Manhattan, Kansas 66506-2601, USA*
[2]*Centre for Quantum Dynamics, Griffith University, Nathan, Queensland 4111, Australia*
[3]*Max-Planck Institut fur Quantenoptik, D-85748 Garching, Germany*

We have used velocity-map imaging to measure the three-dimensional momenta of electrons rescattered from Xe and Ar following the liberation of the electrons from these atoms by 45 fs, 800 nm intense laser pulses. Strong structure in the rescattering region is observed in both angle and energy, and is interpreted in terms of quantitative rescattering (QRS) theory. Momentum images have also been taken with two-color (800 nm + 400 nm) pulses on Xe targets. A strong dependence of the spectra on the relative phase of the two colors is observed in the rescattering region. Interpretation of the phase dependence using both QRS theory and a full solution to the time-dependent Schrödinger equation shows that the rescattered electrons provide a much more robust method for determining the relative phase of the two colors than do the direct electrons.

I. INTRODUCTION

It has been nearly two decades since the now well-known three-step model for describing the interaction of returning electrons, initially extracted by strong laser pulses from atoms, with their parent ion was proposed [1,2]. Electrons removed from the target atom or molecule by the strong field gain energy in that field and return to the ion they left behind with an energy up to $3.2U_p$ (where U_p is the quiver energy of the electron in the field). On their return, they can undergo elastic scattering, inelastic scattering, and radiative capture by the ion. The corresponding laser-induced processes are often called high-energy (or high-order) above-threshold ionization (HATI) [3–5], nonsequential double (and multiple) ionization and high-order harmonic generation, respectively. The basic correctness of the physics of the three-step model is well established, but the quantitative description of the laser processes in terms of the corresponding free-electron processes has only recently been fully exploited. Since the energies of the electrons in the strong-field case are often quite low (tens of eV), conceptually correct models which treat the electron-ion interactions in terms of plane waves are well known to be inadequate quantitatively. However, by factoring the amplitude for the laser process into a product of the full (not plane-wave) scattering amplitude with a "wave packet" representing the effective momentum distribution of the returning electron, recent work has shown that a quantitatively correct description of all three of the laser processes can be achieved. By doing this it becomes immediately possible to apply to the laser problem sophisticated techniques which were developed over many years for the treatment of free-electron collisions. The approach is termed "quantitative rescattering" (QRS) theory [3,5–9]. Related treatments of HATI without the explicit factorization but which include a correct treatment of the electron-ion scattering, have also appeared [4,10,11].

In the first part of this work we describe systematic measurements we have performed, using velocity-map imaging (VMI), of the electron momentum spectra from Xe and Ar at 800 nm over a range of intensities. We have concentrated on the rescattering, or plateau (HATI), electrons whose behavior

is calculable by QRS. The major goal of this part of the work was originally to provide a set of benchmark experimental data for comparison with QRS and to evaluate the successes and shortcomings which are likely to arise in the use of QRS to describe experimental data. A similar benchmark study by Morishita *et al.* [9,12] has recently appeared, and many of the results given here are similar to those presented there. Since that work presented only a single intensity, we focus here on examining to what extent the extracted differential cross sections are independent of the intensity used. Our results were also obtained with a different technique from the one used in that work.

In the second part of this work we describe the use of two-color (800 nm + 400 nm) femtosecond laser pulses to generate the rescattered electrons. The shape of such a pulse resembles closely that at the center of a few-cycle carrier-envelope-phase- (CEP-) stabilized pulse, and much of the physics which attends the use of CEP-stabilized pulses also occurs with the two-color field. The relative phase ϕ of the two colors replaces the CEP in this comparison. The use of two-color fields to study asymmetric ejection of ions and electrons by short laser pulses extends back more than a decade. A major issue over this history has been the determination of the actual phase between the two colors. In the present work, we find that this phase can much more easily and robustly be extracted from the behavior of the rescattered electrons than from the direct electrons. We compare our results to the QRS predictions, and to the results of full, but much more time-consuming, solutions to the time-dependent Schrödinger equation (TDSE). The agreement between theory and experiment is excellent and provides a robust method for assigning the experimental phase.

II. HATI MOMENTUM SPECTRA FROM A SINGLE-COLOR LASER

In a semiclassical description of strong-field ionization [13,14], an electron is extracted from the target at rest and subsequently attains from the laser field an energy ranging up to a maximum of $2U_p$ ("direct" electrons), depending

on the phase of the field at which the electron is created. Higher-energy electrons are produced through rescattering on the ionic core. The returning electrons return with a maximum energy of $3.2U_p$, producing a "plateau" with a final energy ranging up to $10U_p$. A wealth of experimental and theoretical information on these electrons has appeared, of which a sample is found in Refs. [13–25]. One reason for pursuing a quantitative understanding of the rescattering process is the potential of this process for imaging the (time-dependent) structure of the parent ion, especially when it is a molecule. Such an approach is promising due to the high effective flux of the returning electrons [26], much higher than free-electron sources provide.

It was established early that the shape of the plateau [16] and the angular distribution of HATI electrons [15] were target-species dependent. While it seemed clear that such effects were due to the quantitative differences of the differential elastic scattering cross sections for the various targets, only a few quantitative treatments were available [27]. With the development of QRS it is now possible to treat all of these effects quantitatively and economically using free-electron–ion differential scattering cross sections. For example, the different shapes of the plateau for different rare gases [16] are now well explained in terms of the different elastic cross sections for these gases [4,7].

In this paper we concentrate on the angular distributions of the HATI electrons. We begin by briefly summarizing the relevant kinematics of the rescattering electrons [5,6,13]. If the laser electric field and vector potential are given by $E = E_0 \cos(\omega t)$ and $A = -A_0 \sin(\omega t)$ $(E_0 = \omega A_0)$, an electron emitted at $\omega t = 15°$ will return to the target with a maximum rescattering energy of $3.2U_p$, or a momentum (p_r) of $1.2A_0$ (we use atomic units throughout). It can rescatter elastically in the backward hemisphere with this momentum at an angle of θ_r relative to the returning direction. After rescattering the laser will eventually impart to the electron an additional momentum "boost" equal to the value of the vector potential at the time of rescattering, A_r. For ωt of $15°$, the value of A_r is $0.95A_0$. Thus the rescattered electrons from this process will lie on a "back rescattering ridge" (BRR) [3] in momentum space, which is a circle centered at $A_r = 0.95A_0$ with a radius of $1.2A_0$. Thus the ratio between the rescattering momentum p_r and the subsequent "boost" A_r is given by [5,6]

$$p_\gamma = 1.26|A_\gamma|. \tag{1}$$

This relationship determines the aspect ratio of the BRR.

In the QRS treatment, the momentum space distribution of the electrons can be factored into a product of a "wave packet" and a differential scattering cross section [3,5,6]:

$$D(p,\theta) = W(p_r)\,\sigma(p_r,\theta_r). \tag{2}$$

Here $\sigma(p_r,\theta_r)$ is the differential cross section for the scattering of a free electron from the parent ion, $W(p_r)$ is the momentum space distribution characterizing the returning electron, and p and θ are the laboratory momentum polar coordinates of the electron. $W(p_r)$ can be quite complex and depends on the properties of the laser pulse (intensity, pulse length, wavelength, CEP, and so on) but is not a function of θ_r nor is it target-species dependent [5,6]. It can even be defined

so as to include the effects of intensity variation over the focal volume of the experiment [5,6]. Since the purpose of this paper is the extraction of $\sigma(p_r,\theta_r)$, we are not concerned here with the form of $W(p_r)$ but only that it be a unique function of p_r. The laboratory momentum coordinates of the observed electron are related to p_r and θ_r by

$$P_z = A_r - P_r \cos(\theta_r) = P_r \left[1/1.26 - \cos(\theta_r)\right], \tag{3a}$$

$$p_y = p_r \sin(\theta_r). \tag{3b}$$

Morishita *et al.* [3] initially showed that, for rare gases, one could expect marked diffraction structure in $D(p,\theta)$ caused by corresponding structure in $\sigma(p_r,\theta_r)$ along the BRR, and this was confirmed experimentally [28–30]. Experimental values for $\sigma(p_r,\theta_r)$ were extracted from the measured momentum spectra for p_r lying along the BRR only, and good agreement with calculated values of $\sigma(p_r,\theta_r)$ were found. It was later suggested that the kinematic relationship between p_r and A_r given by Eq. (1) should approximately hold for *any* value of p_r [5,6], not only on the BRR. That is, electrons created at ωt other than $15°$, which produce a final p inside the BRR, will also lie on similar circular ridges inside the BRR with the aspect ratio given by Eq. (1), and thus for a given laser intensity the entire momentum distribution $D(p,\theta)$ can be interpreted in terms of Eqs. (1) and (2), extending over a range of p_r values ranging from the BRR value down. In order to avoid contamination from the direct electrons, application of this equation in the region between $4U_p$ and $10U_p$ was suggested to be valid [5,6]. The original data of Okunishi *et al.* [29] were then reanalyzed in these terms, and values of $\sigma(p_r,\theta_r)$ for Ne, Ar, Kr, and Xe were extracted over a range of p_r between 0.8 and 1.2 a.u. Good agreement between theoretical and experimental values of $\sigma(p_r,\theta_r)$ was found [9,12].

The validity of this extraction of $\sigma(p_r,\theta_r)$ from the entire HATI spectrum $D(p,\theta)$ depends on the universality of Eq. (1). If this relationship holds, then for any laser intensity $\sigma(p_r,\theta_r)$ can be extracted from $D(p,\theta)$ for all values of p_r ranging from the BRR value down. Furthermore, for any given p_r, the extracted $\sigma(p_r,\theta_r)$ should be independent of the intensity at which the spectrum was taken. Indeed, a great simplification which results from Eq. (1) is that volume-integral effects do not interfere with the extraction of $\sigma(p_r,\theta_r)$. Any observed (p,θ) corresponds to a unique (p_r,θ_r), regardless of the volume element from which it originated. In this work we concentrate on an investigation of the dependence of the extracted $\sigma(p_r,\theta_r)$ on the laser intensity before proceeding to a comparison of our results with theory.

A. Experiment

The experiments were carried out using a VMI spectrometer [31]. A 45 fs laser pulse with central wavelength at 800 nm and a repetition rate of 1.5 kHz was used. The collimated laser beam was directed into the spectrometer chamber through a 1-mm-thick antireflection-coated glass window and was focused back onto an effusive gas jet by a spherical mirror of focal length 7.5 cm. The ejected electrons were momentum focused onto a multichannel-plate– (MCP-) phosphor screen assembly. The images were captured by a high-resolution camera focused on the back of the phosphor screen through a viewing window. A typical Xe raw momentum image is
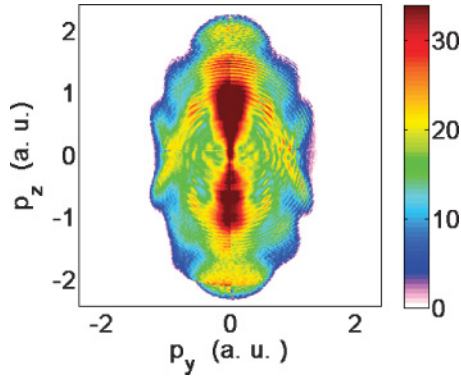
FIG. 1. (Color online) VMI electron momentum image after inversion from Xe target using two-color laser pulses at an intensity of 8.8×10^{13} W/cm^2 (800 nm pulse intensity).

shown in Fig. 1. The raw images are projections of the three-dimensional (3D) momentum distributions. In order to extract a momentum slice from it in the plane of the laser polarization and perpendicular to the laser propagation, the data were Abel inverted [32].

B. Results and discussion

The images for Xe and Ar are shown in Figs. 2 and 3, respectively. Data were taken for up to five laser intensities for most cases [33], but figures are shown here for only three. The left-hand column shows the inverted momentum

images. Since the focus of this paper is on the rescattering region, we block out that part of the spectrum corresponding to electrons with energies below $4U_p$. The strong diffraction structure in the angular distributions is immediately visible. The detector efficiency as a function of position was measured and the momentum spectra were corrected for this. Small ghost artifacts, which do not affect the later discussion, were introduced by this procedure and appear in some of the images for large momenta along $p_z = 0$. Since the major point of presenting these images is to investigate to what extent the entire spectrum, not just the BRR, can be treated in terms of QRS, we present the same data in the central column of Figs. 2 and 3 in terms of the returning electron momentum p_r and free-electron scattering angle θ_r, using Eqs. (3a) and (3b). The energy spectra along the polarization direction (integrated over 10° about the polarization) are shown in the third column of Figs. 2 and 3. The intensities are assigned *in situ* by assigning the observed "cutoff" energies to $10U_p$. These assignments were checked against several other methods, including a "first principles" assignment using the known power, geometry, and pulse length, the measured proton momentum distributions from the same laser pulses on H$_2$, and circular polarization [34], and the results were consistent with those assigned here, but within substantial error bars. We believe the *in situ* assignment of the intensities to be the most reliable, since this procedure assigns an effective intensity which partially accounts for volume averaging of the intensity [4,5]. There is some ambiguity in exactly where the $10U_p$ cutoff should be assigned in the energy spectra, but the error associated
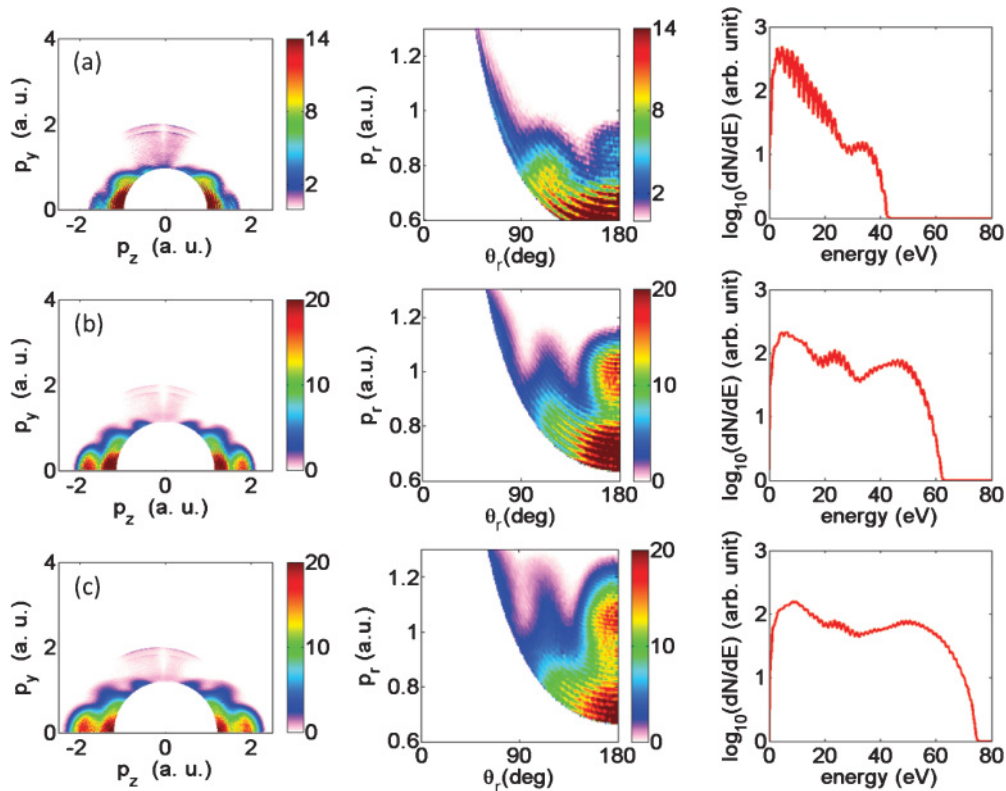

FIG. 2. (Color online) Left-hand column: Inverted electron momentum spectra from Xe for laser intensities of (a) 5.5, (b) 7.7, and (c) 10.0 (in units of 10^{13} W/cm^2). Events with energies less than $4U_p$ are not plotted. Middle column: the same data plotted in terms of p_r and θ_r. Right-hand column: Energy spectra for electrons within a 10° angle of the polarization vector.
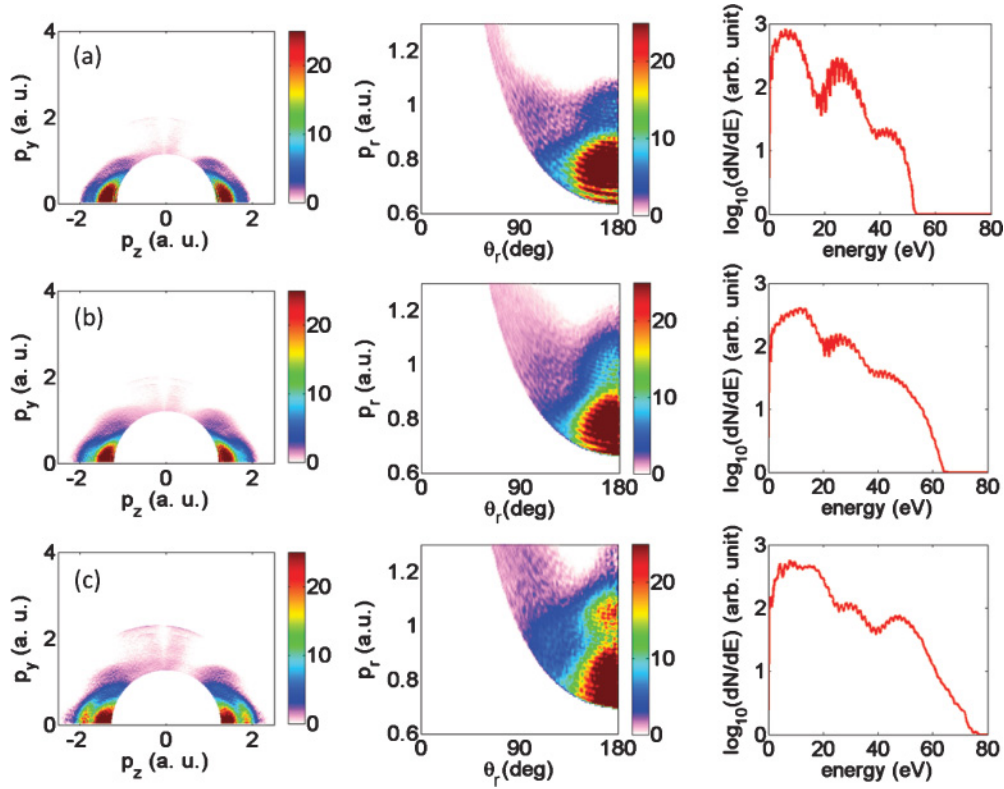
FIG. 3. (Color online) Similar to Fig. 2, but for Ar at intensities of (a) 7.7, (b) 10.0, and (c) 12.8 (in units of 10^{13} W/cm^2).

with this is less than 10% typically, especially when one uses Xe for which the cutoff is very marked. Our assignments are consistent with theoretical energy spectra [3,4].

Angular differential cross sections $\sigma(p_r,\theta_r)$ extracted from the central column images of Figs. 2 and 3 (as well as intensities not shown in Figs. 2 and 3) are shown in Figs. 4 and 5. We have averaged over momentum bins (± 0.03 a.u. around each p_r) to smooth the ATI structure visible in Figs. 2 and 3. Since we do not know $W(p_r)$, and the absolute value of this factor is very intensity dependent, we normalize the experimental $\sigma(p_r,\theta_r)$ extracted for each intensity to approximately make the heights of the curves for different intensities equal. Each value of p_r is related to the equivalent free-electron scattering energy by $E_r = p_r^2/2 : p_r = 1.0$ a.u. corresponds to the scattering of a 13.6 eV electron from the ion. For a given value of p_r, angular distributions can be extracted for any intensity for which this p_r is substantially populated. That is, $3.2U_p$ must equal or exceed E_r. To the extent that QRS is valid, the $\sigma(p_r,\theta_r)$ extracted should be independent of intensity. It is seen that this is nearly true for most cases, thus supporting the claim that Eq. (1) is universal. For small values of p_r one runs the risk that the direct electrons can overlap the rescattering electrons. For example, for $p_r = 0.8$ a.u. in Fig. 4 for Xe, this is apparently the case, since the spectra for two different intensities differ visibly. Generally speaking, for a given p_r it is more reliable to extract $\sigma(p_r,\theta_r)$ from the spectrum with the lowest practical intensity in order to avoid possible contamination of the HATI spectrum with direct electrons.

In Fig. 5 we show a comparison between our experimental values of $\sigma(p_r,\theta_r)$ and those calculated for two different

potentials, "Green" [35] and "Tong" [36]. The experimental curves shown here are taken for the lowest-intensity curve for each value of p_r in Fig. 4, smoothed to remove the ATI structure. The agreement of experiment and theory is by and large good, but the theory shows enough disagreement with the experiment that it is clear that information concerning the correct potential for the electron-ion scattering can be deduced from the strong-field experiments. For example, the exact location of the minima for the case of Xe is not quite correct for either potential used. It appears that information on the ion-electron interaction is available from the strong-field data. This idea has already been exploited by Morishita *et al.* [9] for the rare gases; they used the $\sigma(p_r,\theta_r)$ extracted from the data of Okunishi *et al.* [12,28] to deduce the optimal parameters for the assumed effective electron scattering potential.

Finally we comment briefly on the energy distributions shown in the right-hand column of Figs. 2 and 3. In terms of QRS language, there are two possible sources of structural features in these spectra, one from $W(p_r)$ and one from $\sigma(p_r,\theta_r)$. Local minima in the spectra near laboratory electron energies of 20 eV and 40 eV, weakly intensity dependent, appear in nearly all the spectra. These can be attributed to structure in $W(p_r)$, which has numerous minima. Such minima are not target-species dependent and this appears to be roughly in agreement with our spectra, since they appear for both Xe and Ar. The exact location and shape of theoretical minima in $W(p_r)$ are dependent on the laser characteristics, particularly the pulse length [5,6]. Roughly, these minima can result from interferences between different trajectories contributing to the same p_r. The number of interfering trajectories, and thus the contrast of the minima in $W(p_r)$, is pulse-length dependent.
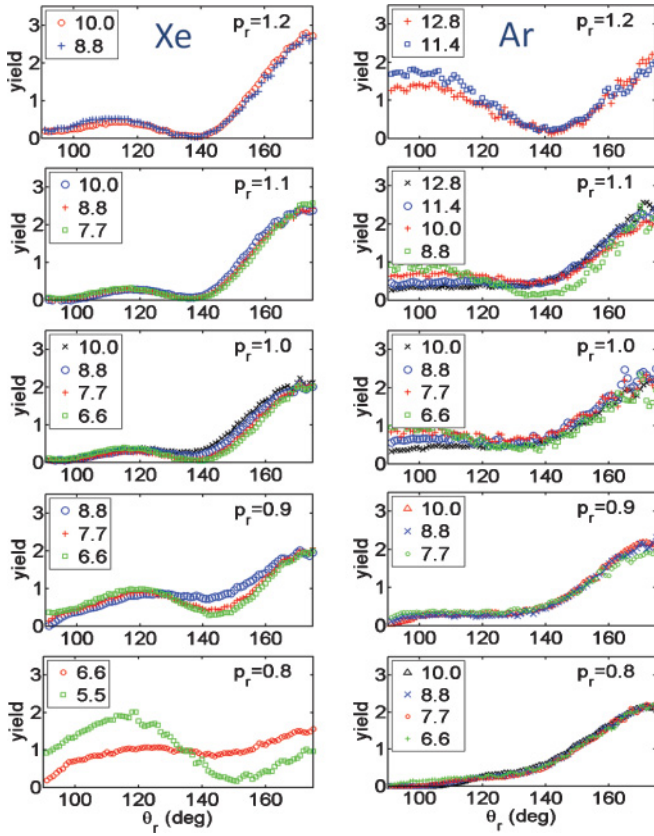
FIG. 4. (Color online) Angular distributions $\sigma(p_r,\theta_r)$ extracted from the middle columns of Figs. 2 and 3 (with additional intensities added). The left-hand column is for Xe, the right-hand one for Ar. The value of p_r in a.u. is given in each figure. The laser intensities, in units of 10^{13} W/cm^2, are shown in the insets.

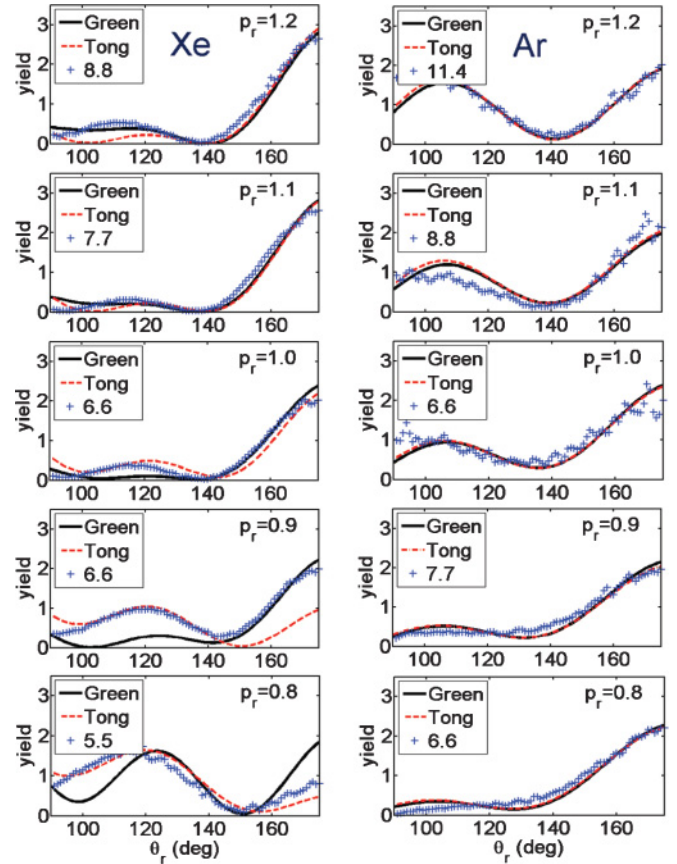FIG. 5. (Color online) Comparison of the angular distributions $\sigma(p_r,\theta_r)$ from Fig. 4 with theoretical calculations from two different electron-ion potentials for different values of p_r. The experimental data for this comparison have been smoothed to remove the ATI structure. The laser intensities, in units of 10^{13} W/cm^2, are shown in the insets.

There is an alternative language: similar energy structure has been known for some years and attributed to "channel closings" [10,11]. Milosevic *et al.* [4] have recently carried out a theoretical analysis of this structure for the rare gases and compared their results to experimental data, and have discussed their results in the channel-closing language. Our data are in agreement with these results.

In the case of Xe, there is an additional minimum in $\sigma(p_r,\theta_r)$ for an electron energy near 30 eV ($p_r = 0.8$ a.u.) [4,7]. This minimum is visible in both the energy spectra and the middle column spectra of Fig. 2. It does not move with intensity. Because it accidentally overlaps with one of the minima in $W(p_r)$, it is difficult to see it separated from the latter minimum, but it remains fixed in energy as the intensity increases while the latter minimum moves slightly to higher energy. This minimum is specific to Xe among the rare gases, and is the main reason Xe gives the most marked plateau of the rare gases [4,7,16].

III. TWO-COLOR EXPERIMENTS

It was established more than a decade ago that the use of a coherent two-color field (ω plus 2ω) will cause the strong-field

ejection of electrons from a target to display a "left-right" asymmetry [37–44]. If the field in the z direction is given by

$$E(t) = E_1 \cos(\omega t) + E_2 \cos(2\omega t + \phi) \qquad (4)$$

(where E_1 and E_2 are the amplitudes of the ω and 2ω components, respectively), the asymmetry of the field evolves as a function of ϕ as shown in Fig. 6(a), displaying a maximally asymmetric field for $\phi = 0, \pi$. One might "intuitively" expect that strong-field ejection of direct electrons for $\phi = 0$ would be preferentially in the negative z direction (the electron is negatively charged). Indeed, maximum emission of the electrons will launch the electrons in this direction, but the direction in which the electron will finally be observed is given by the value of the vector potential at the time of emission, not the electric field. Because the vector potential is passing through zero when the electric field maximizes, the asymmetry of emission will depend on small differences between the time dependence of the vector potential before and after the maximum of the field. A measurement of the directions of emission of both the direct electrons and ions (from a H$_2$ target) was discussed in [42–44] in terms of the "intuitive" directions of emission. This problem was analyzed theoretically by several groups [45–50]. One conclusion [49,50] was that the asymmetry of emission of the direct electrons for a maximally
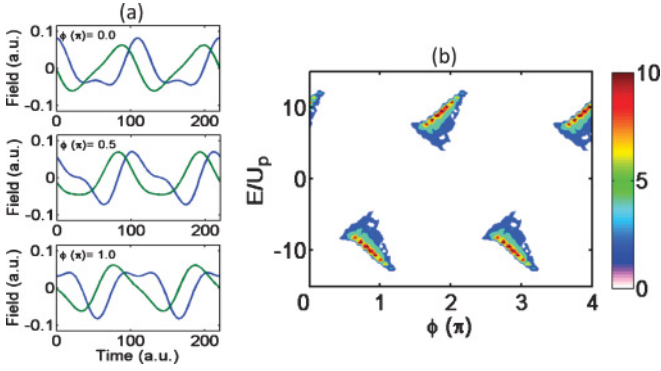
FIG. 6. (Color online) (a) Wave form for a two-color field given by Eq. (4) for various values of the relative phase. [Electric field (blue); vector potential (green).] (b) Results of classical ADK model described in the text. Positive values of E/U_p correspond to the emission of electrons in the negative z direction.

asymmetric field is finite but small and not "intuitive." Thus there appears to be no simple and intuitive way to determine ϕ from a measurement of the asymmetry of emission of the direct electrons.

On the other hand, the direction of emission of the rescattered electrons has a much more intuitive and robust interpretation. Referring to Fig. 6(a), electrons emitted at the peak of the field for $\phi = 0$ will leave in the negative z direction and return, moving in the positive z direction, at a time when the vector potential is nearly maximum (see the discussion above). If they then rescatter in the backward direction from the target, both the rescattering and the additional vector potential "boost" will direct the electrons in the negative z direction. For the rescattering electrons, the emission will thus be robustly "intuitive": the observed electrons will be in the direction of the maximal force on the electron at the time of emission.

To make this qualitative classical discussion somewhat more quantitative, we have performed a classical model calculation. For the electric field given in Eq. (4), for a fixed value of ϕ, we calculate the Ammosov-Delone-Krainov (ADK) [51] emission rate as a function of time. For each emission time, we calculate the classical return time and energy and the vector potential at this time [5,13]. We use these values to calculate the final energy E with which the electron will finally emerge after a 180° scattering. We populate a two-dimensional spectrum of this probability as a function of the rescattering energy and ϕ. The resulting spectrum for an intensity of 10^{13} W/cm^2 and $E_2/E_1 = 0.33$ is shown in Fig. 6(b), where positive values of E/U_p correspond to scattering in the negative z direction, that is, the direction in which the electron is initially removed for an electric field in the positive z direction. As expected, the asymmetry of emission is pronounced and intuitive. Maximal asymmetry occurs near $\phi = 0$ and π. It can also be seen, however, that the maximum energy of the rescattered electron does not occur for $\phi = 0$ and π but at approximately 50° past this phase. This somewhat less intuitive result comes from the fact that the final rescattering energy is determined not by the launch field but by the time integral of the field following launch. These results suggest that a plot of the rescattering energy as a function of two-color phase, if combined with a comparison
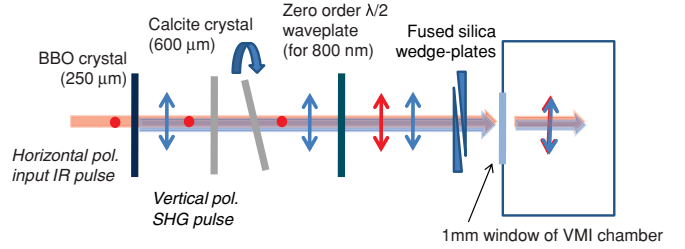
with a theoretical calculation, could be used to extract the absolute phase of the two colors as well as the ratio E_2/E_1. We now proceed to demonstrate this experimentally.

FIG. 7. (Color online) Schematic of two-color setup.

A. Experiment

We generated a two-color field using the collinear setup shown in Fig. 7. A horizontally polarized 45 fs pulse with central wavelength at 800 nm was passed through a 250 μm β barium borate (BBO) crystal which generated a second harmonic 400 nm component due to its nonlinear properties. This 400 nm field has vertical polarization, and also is delayed from the 800 nm pulse by about 60 fs. Both 800 nm and 400 nm pulses were subsequently passed through a zero-order quartz plate which acts as a half-wave plate for 800 nm and rotates its polarization by 90°, but acts as a full wave plate for 400 nm, so that the beam exiting the quartz plate has both components with polarization along the vertical. A 600 μm birefringent calcite crystal was placed between the BBO and the quartz plate to compensate the delay between the two pulses such
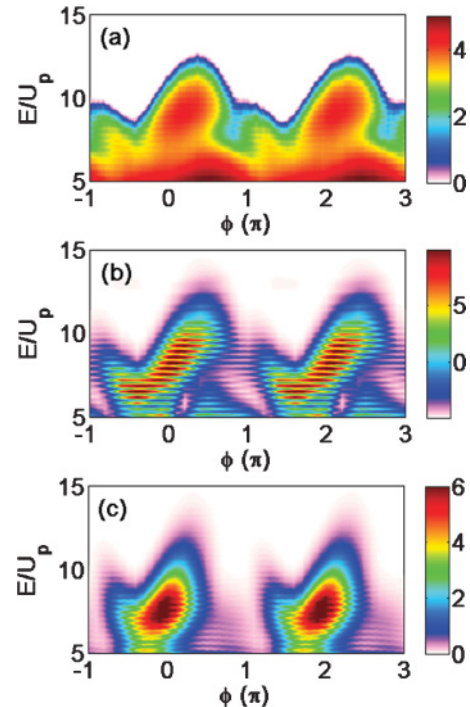

FIG. 8. (Color online) Density plots of the yield of HATI electrons in the negative z direction from Xe as a function of the two-color phase ϕ. (a) Experimental result. (b) TDSE theoretical calculation. (c) QRS volume-integrated result. See text for details.
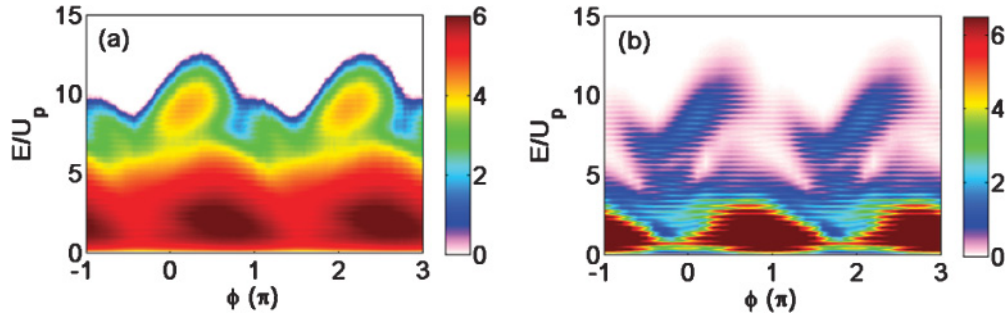
FIG. 9. (Color online) Similar to Fig. 7 but extended in scale to include the direct electrons. (a) Experiment; (b) TDSE calculation.

that they exactly overlapped where the beam was focused on the gas jet. The relative phase between the 800 nm and 400 nm pulses was controlled by rotating the calcite crystal about an optical axis using a motorized rotation stage. A spherical mirror of focal length 75 mm was used to focus the pulses to intensities of $(0.5–2.0) \times 10^{14}$ W/cm^2 onto a neutral Xe gas jet. The momentum spectra were recorded with the VMI setup described above.

B. Results and discussion

For each value of ϕ the inverted VMI spectra were integrated over an angle of 30° about the polarization (z) axis and the energy spectrum (dN/dE) was calculated. A compilation of such spectra for different phases generates a dN/dE distribution plot as a function of energy and phase. Figure 8(a) shows the resulting spectrum for photoelectrons ejected in the negative z direction. Since we are interested only in the HATI electrons at this point, we show electron energies only above $5U_p$. It is sufficient to focus on the variation of the rescattering toward any one side, since the other side can be obtained trivially by shifting ϕ by π. The qualitative behavior of the experimental spectrum resembles that of the model calculation in Fig. 6(b), with a "hooklike" energy feature terminating in a maximum rescattering energy, followed by a region nearly π in extent with low HATI yield.

We compare the experimental result with two theoretical calculations. Figure 8(b) shows the results of a full TDSE calculation for a peak intensity (of the 800 nm component) of 0.6×10^{14} W/cm^2 and E_2/E_1 ratio of 0.3. Because this calculation is very time consuming, a 10 fs pulse length was used instead of the experimental 45 fs. Figure 8(c) shows a QRS calculation with the same parameters but for a peak intensity of 0.76×10^{14} W/cm^2. Because the QRS calculation is much faster, it was practical to perform the explicit volume integral, taking into account the variation of the intensity of both field components assuming Gaussian beam profiles. A slightly higher intensity for the QRS case was used because the volume integral effectively lowers the observed apparent peak intensity [4,5]. The choice of E_2/E_1 in the theoretical calculation was selected to match the experimental results, and thus serves to effectively measure *in situ* this field ratio. We also performed *a priori* measurements of this ratio based on the known power and estimated pulse length and focusing geometry of each component. The results are consistent with the value extracted from the calculation, although within very large error bars. To control all of these parameters with high

precision is nearly impossible, and we consider the *in situ* value to be the most reliable. A very reliable assignment of the absolute phase of ϕ given on the experimental curves is possible by matching the experimental data to the theoretical calculation. As a rule of thumb, assigning the maximum rescattering energy to 50° past $\phi = 0$ is approximately correct, although this result is dependent on the field ratio.

Having assigned ϕ on the basis of the HATI electrons, we can return to examine the behavior of the direct electrons. Figure 9 shows extensions of Figs. 8(a) and 8(b) into the direct electron region on a scale which does not saturate the direct electrons. For both experiment and theory the negative z direct electrons do not maximize in yield for $\phi = 0$ as the intuitive direction would suggest, but rather nearer $\phi = 0.8\pi$. It appears that the behavior of the direct electrons in a two-color field is neither particularly simple nor obvious, a conclusion also reached in Refs. [49,50], and that using them to assign ϕ is at best risky.

IV. SUMMARY AND CONCLUSION

In this paper we have presented experimental evidence establishing the validity of the QRS theory not only for the BRR electrons but over a range of HATI energies between $4U_p$ and $10U_p$. We have observed strong angular structure in the rescattered photoelectron momentum distributions from Xe and Ar. These structures exhibit a strong target structure dependence. The angular differential cross sections as a function of the ion-electron scattering energy were extracted from the data using the QRS formalism. The results were found to be independent of the experimental intensity over a substantial range of intensities. The distributions were compared to differential cross sections calculated from two different potentials, and were found to agree in appearance but, for Xe, not in detail. This result supports the position that characteristics of the electron-ion scattering can be deduced from strong-field laser data [9].

HATI spectra from Xe for two-color (800 and 400 nm) femtosecond laser pulses were studied. The rescattering electron energy was found to have a marked dependence on the relative phase ϕ of the two colors. The asymmetry of the yield was found to be intuitive in the sense that the emission of HATI electrons is favored in the direction that the asymmetric shape of the wave form would suggest. The maximum HATI energy is not found for the value of ϕ that gives the maximum wave-form asymmetry, however. A good agreement between

experimental measurements of the rescattering energy in the polarization direction and theoretical calculations based on both TDSE and QRS formulations was found. Comparison of experiment and theory allows a very reliable assignment of the absolute phase of ϕ in the experiment. The dependence on ϕ of the yield of the direct electrons does not seem to exhibit a simple or intuitive behavior.

[1] P. B. Corkum, Phys. Rev. Lett. **71**, 1994 (1993).

[2] K. J. Schafer, Baorui Yang, L. F. DiMauro, and K. C. Kulander, Phys. Rev. Lett. **70**, 1599 (1993).

[3] T. Morishita, A.-T. Le, Z. Chen, and C. D. Lin, Phys. Rev. Lett. **100**, 013903 (2008).

[4] D. B. Milošević, W. Becker, M. Okunishi, G. Prüumper, K. Shimada, and K. Ueda, J. Phys. B: At. Mol. Opt. Phys. **43**, 015401 (2010).

[5] Z. Chen, A. T. Le, T. Morishita, and C. D. Lin, Phys. Rev. A **79**, 033409 (2009).

[6] C. D. Lin, Anh-Thu Le, Zhangjin Chen, and Toru Morishita, J. Phys. B **43**, 122001 (2010).

[7] Z. Chen, A.-T. Le, T. Morishita, and C. D. Lin, J. Phys. B **42**, 061001(2009).

[8] Z. Chen, T. Morishita, A.-T. Le, and C. D. Lin, Phys. Rev. A **76**, 043402 (2007).

[9] T. Morishita, T. Umegaki, S. Watanabe, and C. D. Lin, J. Phys. Conf. Ser. **194**, 012011 (2009).

[10] A. Čerkić, E. Hasović, D. B. Milošević, and W. Becker, Phys. Rev. A **79**, 033413 (2009).

[11] D. B. Milošević, E. Hasović, M. Busuladžić, A. Gazibegović-Busuladžić, and W. Becker, Phys. Rev. A **76**, 053410 (2007).

[12] T. Morishita, M. Okunishi, K. Shimada, G. Prümper, Z. Chen, S. Watanabe, K. Ueda, and C. D. Lin, J. Phys. B **42**, 105205 (2009).

[13] G. G. Paulus, W. Becker, W. Nicklich, and H. Walther, J. Phys. B **27**, L703 (1994).

[14] W. Becker *et al.*, Adv. At. Mol. Opt. Phys. **48**, 35 (2002).

[15] Baorui Yang *et al.*, Phys. Rev. Lett. **71**, 3770 (1993).

[16] G. G. Paulus, W. Nicklich, Huale Xu, P. Lambropoulos, and H. Walther, Phys. Rev. Lett. **72**, 2851 (1994).

[17] G. G. Paulus, W. Becker, W. Nicklich, and H. Walther, J. Phys. B **27**, L703 (1994).

[18] G. G. Paulus, W. Nicklich, and H. Walther, Europhys. Lett. **27**, 267 (1994).

[19] W. Becker, A. Lohr, and M. Kleber, J. Phys. B **27**, L325 (1994).

[20] G. G. Paulus, W. Becker, and H. Walther, Phys. Rev. A **52**, 4043 (1995).

[21] M.P. Hertlein, P. H. Bucksbaum, and H.G. Muller, J. Phys. B **30**, L197 (1997).

[22] G. G. Paulus, F. Zacher, and H. Walther, Phys. Rev. Lett. **80**, 484 (1998).

[23] M. J. Nandor, M. A. Walker, and L. D. Van Woerkom, J. Phys. B **31**, 4617 (1998).

[24] J. Z. Kaminski and F. Ehlotzky, Phys. Rev. A **55**, 4625 (1997).

[25] Jingtao Zhang *et al.*, J. Phys. B **35**, 4809 (2002).

[26] H. Niikura *et al.*, Nature (London) **417**, 917 (2002).

[27] M. B. Gaarde *et al.*, Phys. Rev. Lett. **84**, 2822 (2000).

[28] M. Okunishi, T. Morishita, G. Prümper, K. Shimada, C. D. Lin, S. Watanabe, and K. Ueda, Phys. Rev. Lett. **100**, 143001 (2008).

[29] D. Ray *et al.*, Phys. Rev. Lett. **100**, 143002 (2008).

[30] S. Micheau, Z. Chen, A.-T. Le, J. Rauschenberger, M. F. Kling, and C. D. Lin, Phys. Rev. Lett. **102**, 073001 (2009).

[31] M. F. Kling *et al.*, New J. Phys. **10**, 025024 (2008).

[32] M. J. J. Vrakking, Rev. Sci. Instrum. **72**, 4084 (2001).

[33] D. Ray, Ph.D. thesis, Kansas State University, 2010.

[34] A. S. Alnaser, X. M. Tong, T. Osipov, S. Voss, C. M. Maharjan, B. Shan, Z. Chang, and C. L. Cocke, Phys. Rev. A **70**, 023413 (2004).

[35] R. H. Garvey, C. H. Jackman, and A. E. S. Green, Phys. Rev. A **12**, 1144 (1975).

[36] X. M. Tong and C. D. Lin, J. Phys. B **38**, 2593 (2005).

[37] C. E. Chen, Y.-Y. Yin, and D. S. Elliott, Phys. Rev. Lett. **64**, 507 (1990).

[38] C. E. Chen and D. S. Elliott, Phys. Rev. Lett. **65**, 1737 (1990).

[39] S. M. Park, S.-P. Lu, and R. J. Gordon, J. Chem. Phys. **94**, 8622 (1991).

[40] D. W. Schumacher, F. Weihe, H. G. Muller, and P. H. Bucksbaum, Phys. Rev. Lett. **73**, 1344 (1994).

[41] G. G. Paulus, W. Becker, and H. Walther, Phys. Rev. A **52**, 4043 (1995).

[42] B. Sheehy *et al.*, Phys. Rev. Lett. **74**, 4799 (1995).

[43] M. R. Thompson *et al.*, J. Phys. B **30**, 5755 (1997).

[44] J. H. Posthumus *et al.*, Phys. Rev. A **54**, 955 (1996).

[45] G. G. Paulus *et al.*, Phys. Rev. Lett. **91**, 253004 (2003).

[46] E. Charron *et al.*, J. Chem. Phys. **103**, 7359 (1995).

[47] E. Charron, A. Giusti-Suzor, and F. H. Mies, Phys. Rev. Lett. **75**, 2815 (1995).

[48] T. Zuo and A. D. Bandrauk, Phys. Rev. A **54**, 3254 (1996).

[49] A. D. Bandrauk and S. Chelkowski, Phys. Rev. Lett. **84**, 3562 (2000).

[50] S. Chelkowski *et al.*, Phys. Rev. A **63**, 023409 (2001).

[51] M. V. Ammosov, N. B. Delone, and V. P. Krainov, Zh. Éksp. Teor. Fiz. **91**, 2008 [Sov. Phys. JETP **64**, 1191 (1986)].